Measurement of a Large Chemical Reaction Rate between Ultracold Closed-Shell ^{40}Ca Atoms and Open-Shell ^{174}Yb^{+} Ions Held in a Hybrid Atom-Ion Trap

Wade G. Rellergert, Scott T. Sullivan, Svetlana Kotochigova, Alexander Petrov, Kuang Chen, Steven J. Schowalter, and Eric R. Hudson

Phys. Rev. Lett. **107**, 243201 — Published 7 December 2011

DOI: 10.1103/PhysRevLett.107.243201

Measurement of a large chemical reaction rate between ultracold closed-shell atoms and open-shell ions held in a hybrid atom-ion trap

Wade G. Rellergert,[1] Scott T. Sullivan,[1] Svetlana Kotochigova,[2] Alexander Petrov,[2,*] Kuang Chen,[1] Steven J. Schowalter,[1] and Eric R. Hudson[1,†]

[1]*Department of Physics and Astronomy, University of California, Los Angeles, California 90095, USA*
[2]*Department of Physics, Temple University, Philadelphia, Pennsylvania 19122, USA*

(Dated: October 21, 2011)

Ultracold $^{174}Yb^+$ ions and ^{40}Ca atoms are confined in a hybrid trap. The charge exchange chemical reaction rate constant between these two species is measured and found to be four orders of magnitude larger than recent measurements in other heteronuclear systems. The structure of the $CaYb^+$ molecule is determined and used in a calculation that explains the fast chemical reaction as a consequence of strong radiative charge transfer. A possible explanation is offered for the apparent contradiction between typical theoretical predictions and measurements of the radiative association process in this and other recent experiments.

PACS numbers:

Interactions between cold ions and atoms have been proposed for use in implementing quantum gates [1], probing quantum gases [2], observing novel charge-transport dynamics [3], and sympathetically cooling atomic and molecular systems which cannot be laser cooled [4, 5]. Furthermore, the chemistry between cold ions and atoms is foundational to issues in modern astrophysics, including the formation of stars, planets, and interstellar clouds [6], the diffuse interstellar bands [7], and the post-recombination epoch of the early universe [8]. However, as pointed out in Refs. [9] and [10], both experimental data and a theoretical description of the ion-atom interaction at low temperatures, reached in these modern atomic physics experiments and the interstellar environment, are still largely missing.

Of particular interest in cold ion-atom physics are binary charge exchange reactions, which limit the performance of the aforementioned proposals and are important inputs to astrophysical models. Binary charge exchange reactions occur via three mechanisms: (i) non-radiative charge transfer (nRCT), $A^+ + B \rightarrow A + B^+$, (ii) radiative charge transfer (RCT), $A^+ + B \rightarrow A + B^+ + \gamma$, and (iii) radiative association (RA), $A^+ + B \rightarrow (AB)^+ + \gamma$. Due to the scarcity of reaction data and full quantum calculations, a number of approximation techniques for these processes have been developed, *e.g.* approximating all RA rate constants by 10^{-14} cm^{3}s^{-1} [11], Landau-Zener theory [12], the Demkov coupling method [13], and the semi-classical optical potential method [14]. These techniques, which have varying degrees of accuracy depending on the dominant charge exchange pathway, must be experimentally verified as demonstrated by a recent measurement where a factor of ∼100 discrepancy was found with experiment [10, 15].

Total charge exchange rate constants have recently been measured for two ultracold ion-atom species [16–18]. In the first system the charge exchange rate constant for the resonant, homonuclear case of $Yb^+ + Yb$ was measured by Grier *et al.* to be $\sim 6\times10^{-10}$ cm^{3}s^{-1} [16], in good agreement with a subsequent theoretical calculation [19]. On the other hand, a measurement of the rate constant for the non-resonant, heteronuclear case of $Yb^+ + Rb$ by Zipkes *et al.* yielded $\sim 3.5\times10^{-14}$ cm^{3}s^{-1} [17]; an experiment on $Ba^+ + Rb$ appears to have yielded similar results [20]. Finally, a calculation of the heteronuclear case $Ca^+ + Na$ yielded 2.3×10^{-16} cm^{3}s^{-1} [4, 21]. These values agree well with conventional wisdom for resonant versus non-resonant charge exchange. Interestingly, although the RA process is typically predicted to be the dominant mechanism for low-temperature, non-resonant charge exchange [22–24], none of the experiments observed the formation of a molecular ion. Further, Zipkes *et al.* found the ratio of the rate of nRCT to RCT to be $K_{nRCT}/K_{RCT} \approx 2.3$, while most calculations predict $K_{nRCT}/K_{RCT} \leq 10^{-3}$ in the ultracold regime [22–24].

Here we report the first measurement of the charge exchange chemical reaction rate constant, K, for the non-resonant, heteronuclear case of a closed shell atom, ^{40}Ca , with an open shell ion, $^{174}Yb^+$, in a hybrid trap. Interestingly, though conventional wisdom says that closed-shell species are less reactive, we find a reaction rate of $K \approx 2 \times 10^{-10}$ cm^{3}s^{-1}, four orders of magnitude larger than measured in open-shell systems. In addition, by monitoring the production of $CaYb^+$ molecular ions in the hybrid trap, we place an apparent upper bound on the branching ratio of the RA process, under the assumption that the produced molecular ions do not experience further chemical reaction. We have also constructed molecular potential curves for the $CaYb^+$ molecule that describe the individual pathways for the reactions and we explain this rate as a consequence of an avoided crossing and similar neutral atom polarizabilities, which yield a large transition dipole moment and large Franck-Condon factors. In what follows, we describe the experimental setup, results, and theoretical model. We conclude with

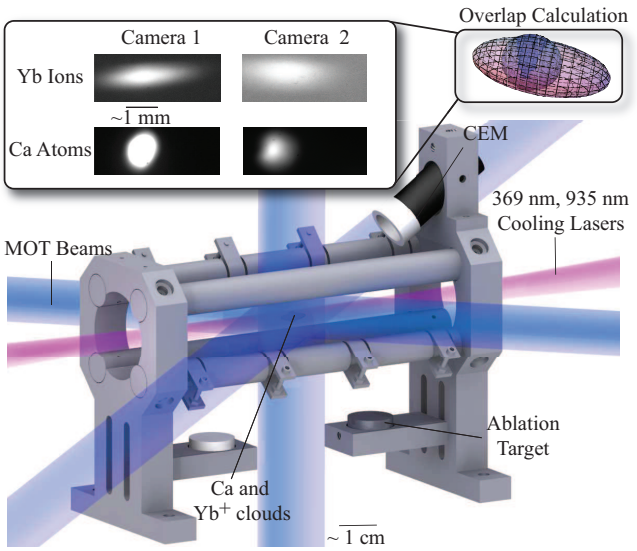

FIG. 1: MOTION trap schematic. Yb^+ ions and Ca atoms are laser cooled and trapped in the central region. Typical images of the ultracold clouds, shown in the upper left of the figure, are used for a 3D reconstruction that yields the degree of overlap. Ions are also detected with a voltage-gated CEM.

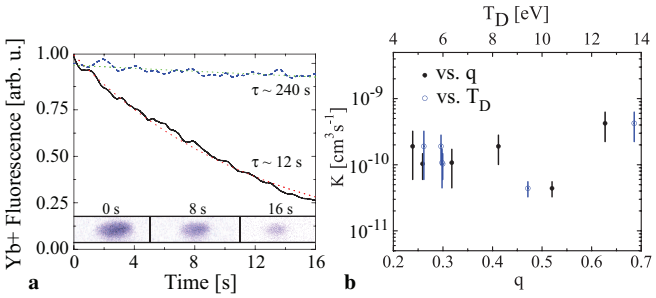

FIG. 2: (a) Yb^+ ion trap lifetime in the presence of the MOT (solid curve) compared to the lifetime without a MOT (dashed curve). Dotted curves are single exponential decay fits. Inset: Images of the Yb^+ ion cloud in the presence of the MOT at various times. (b) Loss rate constant as a function of the Mathieu stability parameter q and the trap depth T_D.

a possible explanation for the apparent contradiction between typical theoretical predictions and measurements of the RA process in this and other experiments [17].

Figure 1 shows the hybrid magneto-optical and ion trap system used in these experiments [5]. Yb^+ ions, created by laser ablation of a solid Yb target, are trapped in a radio-frequency linear quadrupole trap (LQT) [25] (250 kHz $\leq f_{\rm rf} \leq$ 400 kHz, $V_{\rm RF} \approx 300$ V) and laser-cooled using laser beams ($\lambda = 369$ nm, 935 nm) aligned along the trap axis. A voltage-gated channel electron multiplier (CEM) provides a species non-specific method of ion detection. Ultracold Ca atoms are produced and held in a magneto-optical trap (MOT) constructed with laser beams ($\lambda = 422$ nm, 672 nm) that intersect at the LQT center. Fluorescence images of both the Ca MOT and the Yb^+ ion cloud from two separate, nearly orthogonal camera angles allow a 3D reconstruction of the ion and atom clouds. An example of such images and the reconstruction is shown in the inset of Fig. 1.

The typical MOT atom number, density, and temperature are measured by absorption and fluorescence imaging and found to be $N_{\rm Ca} = 3.7 \pm 0.5 \times 10^6$ atoms, $\rho_{\rm Ca} = 7 \pm 1 \times 10^9$ cm^{-3}, and $T_{\rm Ca} = 4 \pm 1$ mK, respectively. Ion number and temperature are determined by observing ion fluorescence while scanning the 369 nm laser ($\dot{f} = 500$ MHz/s) and fitting the resultant truncated Voigt profile [26]. When operating the LQT in a region where both Ca^+ and Yb^+ ions are stable, a large heat load on the laser cooled Yb^+ ions is observed due to the ionization of Ca atoms in the 4^1P state by the Yb^+ cooling laser. To eliminate this effect, we modulate the intensity of the 422 nm and 369 nm lasers out of phase. Additionally, this effect is eliminated if the LQT is operated where Ca^+ ions are not trapped.

In absence of the Ca MOT, the trap lifetime of the laser-cooled Yb^+ ions, measured by monitoring the ion fluorescence, is $\sim$ 240 s. However, when an overlapped MOT is introduced, the ion lifetime decreases to $\sim$ 10 s, as shown in Fig. 2(a). This induced ion loss is also confirmed visually by imaging the ion cloud during the decay, as well as observing a decreased number of detected ions using the CEM. The inset in Fig. 2(a) suggests that the loss of ions is not due to ion heating, as such an effect would increase the ion cloud size. From data such as these we calculate a loss rate constant using $K = \langle \sigma v \rangle = \frac{\Gamma}{\rho \Phi}$, where Γ is the measured fluorescence decay rate, ρ is the peak density of the MOT, and Φ a factor that quantifies the degree of overlap of the atom and ion clouds. We define $\Phi = \int \hat{\rho}_{Ca}(\vec{r}) \bar{\rho}_I(\vec{r}) d\vec{r}$, where $\hat{\rho}_{Ca}$ is the unit-peak normalized Ca atom density and $\bar{\rho}_I$ is the unit-integral normalized Yb^+ density, thus $0 < \Phi < 1$.

To verify that kinematic effects were not responsible for the loss of Yb^+ ions from the trap, we measured the loss rate constant while varying only q, the Mathieu parameter, which determines the ions' stability and micromotion amplitude in the LQT [25], as well as when only varying the trap depth, T_D (see Fig. 2(b)). As the rate constant appears independent of these fundamental trapping parameters, it is unlikely that the loss is due to kinematic effects in the LQT. In addition, we performed an experiment where $BaCl^+$ ions, produced by laser ablation of an additional target (see Fig. 1), were sympathetically cooled by co-trapped, laser cooled Yb^+ ions. We then compared, after 20 s of interaction with the MOT, the number of ions remaining in the trap and found that while the Yb^+ ions had decayed away, the $BaCl^+$ ions remained. As $BaCl^+$ ions are energetically forbidden to charge exchange with Ca atoms [5], we conclude the loss of Yb^+ ions is due to a charge exchange reaction.

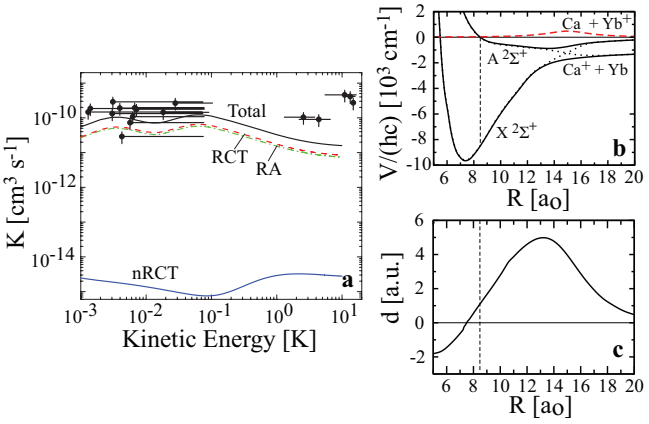

FIG. 3: (a)Total experimental (points) and theoretical (black line) charge exchange rate constants as a function of ion kinetic energy. The horizontal location of the data point is the value of the secular kinetic energy as measured by the Doppler fluorescence technique. The horizontal "error bars" represent the contribution of the micromotion to the overall kinetic energy. Also shown are the calculated rate constants for the three charge exchange pathways. (b) The X $^2\Sigma^+$ and A$^2\Sigma^+$ potential energy curves and (c) the corresponding transition dipole moment of the CaYb$^+$ molecular ion as a function of the internuclear separation R. The dotted curves are the diabatized potentials constructed from these potentials. The dashed curve gives the coupling constant between the diabatic potentials.

After these systematic checks the loss rate constant was measured as a function of kinetic energy, as shown in Fig. 3(a). For these measurements the MOT temperature was held at 4 mK and the ion temperature was varied by changing the cooling laser detuning and intensity. The horizontal "error bars" of this figure represent the contribution of the coherent radial micromotion, not measured by the Doppler fluorescence technique, to the total ion kinetic energy [27]. The micromotion amplitude grows with radial position in the ion cloud and varies from zero on the axis of the trap to the value given by the rightmost tip of the "error bar" at the edge of ion cloud. The observed rate constant is roughly four orders of magnitude larger than typical non-resonant, heteronuclear charge exchange values and is constant within experimental error over all measured temperatures.

We have also experimentally verified that the measured reaction rate constant is the value for ground state atoms and ions. Reactions between excited state atoms and ions have been ruled out by measuring the rate constant while modulating the 422 nm and 369 nm cooling light out of phase. Additionally, we performed measurements of the rate constant as a function of the excited state fraction of both the atoms and ions by separately varying the intensity of their respective cooling lasers. In these measurements we observed the rate constant to be constant within experimental error as a function of both atom and ion excitation fraction, indicating that the reported rate is the value for ground state reactions. It is possible that excited state atom collisions are supressed by the long range atom-ion interaction, which shifts the cooling lasers out of resonance before the particles are close enough to react [16, 28], however, the possibly large micromotion velocity does weaken this argument. Finally, the results of Ref. [28] do not apply to the case of an excited state ion since the ground and excited long range potentials are similar, thus we speculate from the constancy of the rate that excited and ground state ions react at a similar rate, though more investigation is needed.

The charge exchange reaction products can in principle be trapped, but due to the large mass ratio of Ca^+ ($m = 40$ amu) and Yb^+ ($m = 174$ amu) ions, Ca^+ ions are heated by the cold Yb^+ ions [27]. This effect is exacerbated by the fact that trap operation in a mutually stable region necessarily puts one or both ion species near a boundary of their LQT stability region. As a result, at the trap parameters used in this study, Ca^+ ions have a measured trap lifetime of only $\sim$1 s. Given the comparatively low production rate from charge exchange reactions with Yb^+ ions, the equilibrium number of Ca^+ ions in the trap is ≤ 2, which is below our current detection limit. Conversely, the mass of the $CaYb^+$ reaction product is much closer to that of Yb^+ and does not suffer from these effects. Therefore, neglecting further chemical reaction with the Ca MOT, $CaYb^+$ ions are expected to have a trap lifetime of at least that of uncooled $BaCl^+$ ions (m $\sim$ 17 amu) which we measure to be $\sim$30 s. Thus, by allowing the Yb^+ ion fluorescence to decay to background levels, measuring the number of ions remaining in the trap using the CEM, and accounting for systematic effects such as trap loss and mass dependence of the ion detection efficiency, we place an apparent upper limit on the branching ratio for RA at 0.02, under the assumption that all detected ions are $CaYb^+$.

Also shown in Fig. 3(a) are the results of our theoretical model for the charge exchange rate constant. Since the structure of $CaYb^+$ was previously unknown, we first calculated the electronic potential surfaces that dissociate to the Ca+Yb^+ and Ca^++Yb limits, and their transition dipole moment [29], as shown in Fig. 3(b) and (c) (solid curves), respectively. This approach worked well for the structure of the $BaCl^+$ molecular ion [30]. The $CaYb^+$ X $^2\Sigma^+$ and A$^2\Sigma^+$ states are asymptotically separated by an energy splitting of 1136 cm^{-1} [31] with an attractive long-range $-C_4/R^4$ behavior; C_4 is 71.5 a.u for the X $^2\Sigma^+$ state and 78.5 a.u. for A$^2\Sigma^+$ state. The two potentials have an avoided crossing near $R = 15a_0$ with a smallest separation of 946 cm^{-1}. Using these potentials, we calculated the rate constant for the charge exchange pathways via a quantum mechanical scattering calculation that assumed the particles collide on the A$^2\Sigma^+$ potential and charge exchange to bound or continuum states of the X$^2\Sigma^+$ potential.

Since the nRCT pathway occurs via a nonadiabatic transition near the avoided crossing, we determine its rate constant by a coupled-channels method with diabatized potentials – black dotted lines in Fig. 3(b). For the coupling between these potentials, we assume a Lorentzian in R with a maximum value equal to half the minimum splitting of the adiabatic potentials. The width of the coupling matrix element is chosen such that diagonalization of the 2×2 potential matrix reproduces the original adiabatic potentials. To characterize the nature of the coupling, we varied its strength between the diabatic potentials by 20%. Although the nRCT rate coefficient does increase with coupling strength, it does not exceed a few times 10^{-14} cm^{3}s^{-1}, indicating that the scattering is almost adiabatic.

For the calculation of the RCT and RA rate constants, we use Fermi's golden rule for the spontaneous emission of a photon by the diatom. In principle, both the initial and final state wavefunctions are solutions of a two-channel calculation as for nRCT, however, since the scattering is nearly adiabatic, we assume that the initial state is a scattering solution of the $A^2\Sigma^+$ potential and the final state is either a bound or scattering state of the X $^2\Sigma^+$ potential. Thus, the total radiative rate coefficient for an initial Ca+Yb$^+$ energy-normalized state $|\mathrm{A}, \epsilon\ell m\rangle$ with collision energy ϵ, relative angular momentum quantum number ℓ, and projection m is

$$K_{\epsilon\ell m} = \frac{2\pi^2}{\sqrt{2\mu\epsilon}} \sum_f \frac{4}{3}\alpha^3\omega^3_{f,\epsilon\ell}|\langle \mathrm{X}, f|d|\mathrm{A}, \epsilon\ell m\rangle|^2 \qquad (1)$$

where α is the fine-structure constant, μ is the reduced mass, and all quantities are expressed in atomic units. The sum is over final states f, which denote either a continuum wavefunction $|\mathrm{X}, \epsilon'\ell'm'\rangle$ leading to RCT or a ro-vibrational state $|\mathrm{X}, v\ell'm'\rangle$ of the $X^2\Sigma^+$ potential leading to RA. The quantity $\omega_{f,\epsilon\ell}$ is the frequency difference between the initial and final states and the operator d is an abbreviation for $d(R)C_{1q}(\hat{R})$, where $d(R)$ is the R-dependent dipole moment between the X and A state, $C_{1q}(\hat{R})$ is a spherical harmonic, $\hat{R}$ the orientation of the molecule in a space-fixed coordinate system, and $q = m - m'$ gives the polarization of the emitted photon. The selection rules of the dipole moment ensure that $|\ell - \ell'| \leq 1$ and $|m - m'| \leq 1$. Figure 3(a) shows the thermalized radiative rate constants due to both RCT and RA mechanisms versus temperature.

Figure 3(a) also shows the total rate constant which agrees well with the data. Our calculations show that the enhanced rate constant is the result of the avoided crossing of the molecular potentials (Fig. 3(b)), which gives rise to a large transition dipole moment due to the mixing of the states (Fig. 3(c)). Additionally, there is good Franck-Condon overlap due to the similarity of the long range potentials. We speculate that similar systems with avoided crossings (e.g. Ba + Yb$^+$, and Sr + Yb$^+$) might show enhanced rate constants as well.

Although there is satisfactory agreement with the total calculated and measured rate constant, the predicted RA branching ratio of ~ 0.5 strongly disagrees with the measured value ≤ 0.02. These ratios could be reconciled, however, if the CaYb$^+$ further reacted with the Ca MOT atoms via subsequent RA reactions, *e.g.* CaYb$^+$ + Ca → $Ca_2Yb^+ + \gamma$, to form heavier molecular ions, which, due to technical constraints, are unstable in our LQT. Given that RA will predominantly produce CaYb$^+$ in high-lying vibrational states, which are typically very reactive, this explanation seems quite plausible. Further, if the same explanation is applied to the data of Ref. [17], the interpretation of trap loss as evidence of nRCT could be reinterpreted as evidence of RA, yielding a RA branching ratio that agrees well with typical theoretical predictions.

In conclusion, we have presented an experimental and theoretical investigation of the charge exchange reaction of the Ca + Yb$^+$ system. The total measured and calculated rate constants are in good agreement and are surprisingly large for a non-resonant, heteronuclear charge exchange reaction. We have also offered a plausible explanation for the apparent contradiction between typical theoretical predictions and measured rates of RA in this and other experiments. However, the discrepancy between theory and experiment clearly calls for future investigations into molecular ion formation. Given the importance of these types of reactions for determining astrophysical processes, this work highlights the need for fully quantum calculations on a case-by-case basis and a renewed effort in laboratory astrophysics. Finally, we note that chemical reactions such as charge exchange could be a concern for the development of many of the applications of hybrid atom-ion trap systems, and thus, when designing future experiments, the choice of atomic and ionic species must be carefully considered.

This work was supported by NSF grant No. PHY-1005453, ARO grant No. W911NF-10-1-0505 and AFOSR grant. ERH thanks Phillip Stancil for illuminating discussions.

Note – After submission of this manuscript, the RA process was observed in the CaRb$^+$ system [32]. Evidence for further chemical reaction of CaRb$^+$ was observed, supporting our explanation for the apparent lack of RA products in the open-shell CaYb$^+$ system.

* Alternative adress: St. Petersburg Nuclear Physics Institute, Gatchina, 188300; Department of Physics, St.Petersburg State University, 198904, Russia
† Corresponding author: eric.hudson@ucla.edu

[1] Z. Idziaszek, T. Calarco, and P. Zoller, Phys. Rev. A **76**, 033409 (2007).
[2] C. Kollath, M. Köhl, and T. Giamarchi, Phys. Rev. A **76**, 063602 (200).
[3] R. Côté, Phys. Rev. Lett. **85**, 5316 (2000).
[4] W. W. Smith, O. P. Makarov, and J. Lin, J. Mod. Optic. **52**, 2253 (2005).
[5] E. R. Hudson, Phys. Rev. A **79**, 032716 (2009).
[6] D. Smith, Chem. Rev. **92**, 1473 (1992).
[7] V. S. Reddy, S. Ghanta, and S. Mahapatra, Phys. Rev. Lett. **104**, 111102 (2010).
[8] P. Stancil and B. Zygelman, Astrophys. J. **472**, 102 (1996).
[9] Z. Idziaszek et al., Phys. Rev. A **79**, 010702 (2009).
[10] J. Woodall et al., Astron. Astrophys. **466**, 1197 (2007).
[11] J. B. Kingdon, Mon. Not. R. Astron. Soc. **274**, 425 (1995).
[12] S. E. Butler and A. Dalgarno, Astrophys. J. **241**, 838 (1980).
[13] Y. N. Demkov, Sov. Phys. JETP **18**, 138 (1963).
[14] B. Zygelman and A. Dalgarno, Phys. Rev. A **38**, 1877 (1988).
[15] A. Luca, D. Voulot, and D. Gerlich, WDS Proc. of Contrib. Pap., **2**, 294 (2002).
[16] A. Grier et al., Phys. Rev. Lett. **102**, 223201 (2009).
[17] C. Zipkes et al., Nature **464**, 388 (2010).
[18] C. Zipkes et al., Phys. Rev. Lett. **105**, 133201 (2010).
[19] P. Zhang, A. Dalgarno, and R. Côté, Phys. Rev. A **80**, 030703 (2009).
[20] S. Schmid, A. Härter, and J. Denschlag, Phys. Rev. Lett. **105**, 133202 (2010).
[21] O. Makarov, R. Côté, H. Michels, and W. Smith, Phys. Rev. A **67**, 042705 (2003).
[22] B. Zygelman et al., Phys. Rev. A **40**, 2340 (1989).
[23] C. Liu et al., Phys. Rev. A **79**, 042706 (2009).
[24] L. B. Zhao et al., Astrophys. J. **615**, 1063 (2004).
[25] D. J. Douglas, A. J. Frank, and D. Mao, Mass Spect. Rev. **24**, 1 (2005).
[26] D. Kielpinski et al., Opt. Lett. **31**, 757 (2006).
[27] F. G. Major and H. G. Dehmelt, Phys. Rev. **170**, 91 (1968).
[28] Y. B. Band and P. S. Julienne, Phys. Rev. A **46**, 330 (1992).
[29] G. Karlström and *et al.*, Comp. Mat. Sci. **28**, 222 (2003).
[30] K. Chen et al., Phys. Rev. A **83**, 030501 (2011).
[31] Y. Ralchenko, A. Kramida, and J. Reader, NIST Atomic Spectra Database **version 4**, http://physics.nist.gov/asd (2010).
[32] F. H. J. Hall et al., arXiv:1108.3739 (2011).